Analyzing the Structure of CoFe−Fe_3O_4 Core−Shell Nanoparticles by Electron Imaging and Diffraction

Jing Li,[†] Hao Zeng,[‡] Shouheng Sun,[‡] J. Ping Liu,[§] and Zhong Lin Wang*[,†,#]

School of Materials Science and Engineering, Georgia Institute of Technology, Atlanta, Georgia 30332, IBM T. J. Watson Research Center, Yorktown Heights, New York 10598, Department of Physics, University of Texas at Arlington, Arlington, Texas 76019, and National Center for Nanoscience and Nanotechnology, Beijing 100080, China

Received: June 3, 2004; In Final Form: July 3, 2004

Structure analysis of multifunctional nanoparticles could be a complex process. In this paper, we demonstrate the step-by-step techniques used for identifying the structure of the CoFe−Fe_3O_4 nanoparticles, which are composed of ∼4-nm CoFe cores and covered with ∼3-nm Fe_3O_4 polynanocrystallites. The techniques demonstrated are general and can be adopted for analysis of any nanoparticles of interest in physical chemistry.

Core−shell structured nanocrystals are interesting because of their unique physical and chemical properties, as well as their technological applications.[1−9] The core−shell structured nanoparticles have the advantage of tuning and tailoring their physical properties by designing the chemical compositions as well as sizes of the core and the shell.[1−9] The wurtzite CdSe−CdS core−shell semiconductor nanoparticles, for example, show a comprehensively improved photostability, electronic accessibility, and high quantum yield.[3] The ferromagnetic Co nanoparticles enclosed by an antiferromagnetic CoO shell provide an extra source of anisotropy induced by the exchange coupling at the interface between the two phases, leading to enhanced ferromagnetic stability beyond the "superparamagnetic limit".[7] The $Fe_{58}Pt_{42}$−Fe_3O_4 core−shell nanoparticles demonstrate interphase exchange coupling between the core (magnetic hard phase) and the shell (magnetic soft phase), which may lead to magnets with improved energy products.[8]

The physical and chemical properties and performances of the core−shell nanoparticles strongly depend on their microstructure, which includes the structure of the core, the shell, and the interface.[1−3,7,9] The interface is particularly important because its sharpness, lattice mismatch, and chemical gradient are critical for electron transfer and coupling. An epitaxial orientation relationship between the core and the shell is favorable, but an epitaxial growth is determined by their crystal structures.[9] The analysis of the core−shell structure with a coherent interface is relatively simple for high-resolution transmission electron microscopy (HRTEM), but analysis of an incoherent or lattice-unmatched interface for core−shell particles is challenging, due to the small size of the grains as well as the complex orientation.

In this paper, we use the CoFe−Fe_3O_4 nanoparticles as an example to demonstrate the procedures and complimentary techniques to be used for identifying the structures of the nanoparticles. The techniques and methodology demonstrated are general and can be adopted for analysis of any nanoparticles.

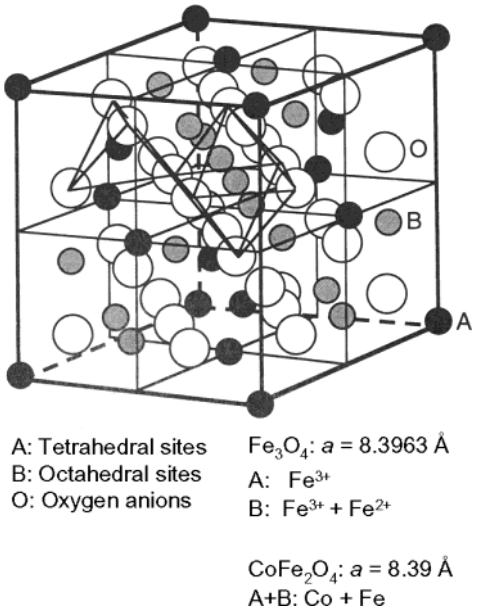

Figure 1. Schematic model of the Spinel unite cell structure.

The CoFe−Fe_3O_4 nanoparticles were obtained by coating iron species over a 4-nm $CoFe_2O_4$ core, synthesized following a published procedure.[10] The coating was performed by mixing the $CoFe_2O_4$ particles with oleic acid, olyel amine, phenyl ether, and $Fe(CO)_5$, and heating the mixture to refluxing. The synthetic details will be published separately. The as-synthesized nanoparticles were deposited on a carbon film supported by a copper grid. HRTEM analysis was carried out at 200 kV using a Hitachi HF-2000 Field Emission TEM and at 400 kV using a JEOL 4000EX TEM.

From the synthesis technique presented above, the most likely structure could be $CoFe_2O_4$ and Fe_3O_4, which have the Spinel structure (as shown schematically in Figure 1) with almost perfect lattice and structure match. The Spinel structure has two cation sites: the tetrahedrally coordinated A sites and the octahedrally coordinated B sites. For Fe_3O_4, the A and B positions are occupied by $Fe^{3+}$and Fe^{2+} cations, respectively. For $CoFe_2O_4$, the A and B positions are equally occupied by Co and Fe cations. Fe_3O_4 and $CoFe_2O_4$ have almost the same

* Corresponding author e-mail: zhong.wang@mse.gatech.edu.
[†] Georgia Institute of Technology, Atlanta.
[‡] IBM Corp.
[§] University of Texas at Arlington.
[#] National Center for Nanoscience and Nanotechnology.

10.1021/jp047602f CCC: $27.50
Published on Web 08/12/2004

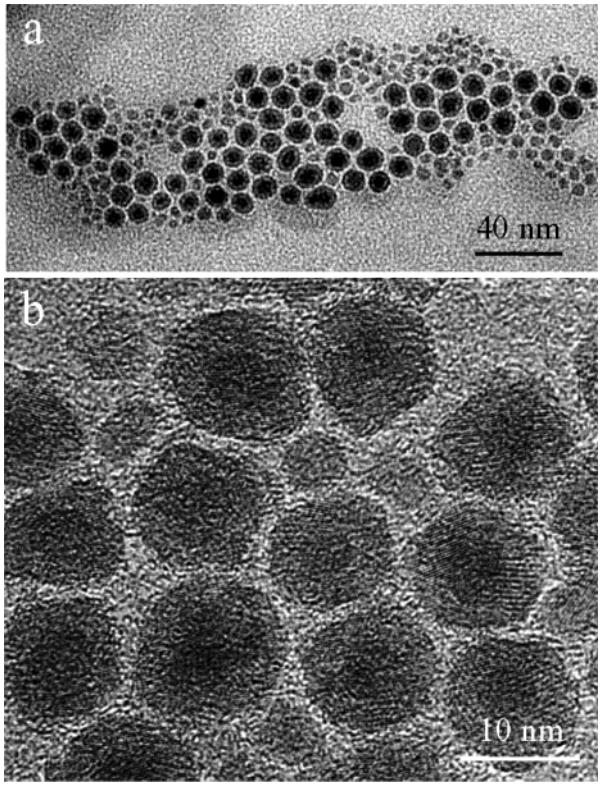

Figure 2. (a) Low-magnification TEM image recorded from monolayer-dispersed nanoparticles, showing a mixture of larger-size core−shell structured nanoparticles and smaller single-phase nanoparticles. (b) Enlarged TEM images showing the polycrystalline shell structure.

lattice parameters: $a = 8.3963$ Å for Fe_3O_4, $a = 8.39$ Å for $CoFe_2O_4$. The mass densities for Fe_3O_4 and $CoFe_2O_4$ are almost identical. Considering the facts of the very small difference in atomic numbers between Co and Fe and the identical crystal structure, the two phases can be hardly distinguished by either HRTEM or X-ray diffraction, especially with the shape-induced peak broadening.

Figure 2a shows a typical low-magnification TEM image of the nanoparticles, which clearly displays the core−shell morphology of 9−10 nm in size. Figure 2b shows an enlarged TEM image showing that the core−shell nanoparticles have a uniform shell, but that the shell is composed of tiny nanocrystallites (so-called polycrystalline). In contrast to the expected result, the core shows a darker contrast than the shell, indicating that the core should have a higher projected mass density. This is impossible if the core is $CoFe_2O_4$ and the shell is Fe_3O_4. The question now is what are the core and the shell?

HRTEM is applied first to determine the structure of the larger-size nanoparticles. Figure 3a shows a typical HRTEM image and corresponding Fourier transformations from the adjacent regions in the shell. The lattice spacing can be directly measured from the image, and the projected symmetry is revealed by the Fourier transformation. The image clearly shows the structure of the shell, but the core is unresolved due to a different crystal orientation. The symmetry of the local image and the interplanar spacing of the shell fit well to the Spinel structure. The shell shows two grains oriented along [114] and [125].

Energy-dispersive X-ray spectroscopy (EDS) is applied to determine if the shell is Fe_3O_4 or $CoFe_2O_4$. By using a fine electron probe of ~3 nm, EDS spectra were acquired by positioning at different parts of the large-size nanoparticle. Figure 4 shows a comparison of EDS spectra acquired by

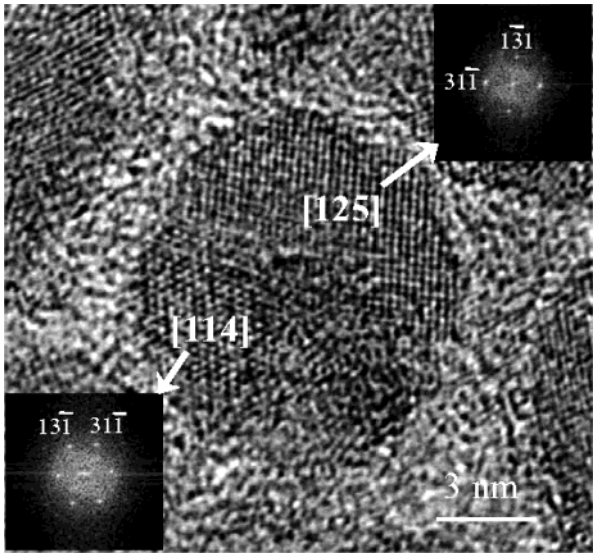

Figure 3. HRTEM image and corresponding Fourier transforms of the image recorded from a large-size core−shell nanoparticle, showing the Spinel structure of the shell. The shell is composed of nanocrystallites; the two that can be identified from the image are oriented along [125] and [114] of Fe_3O_4.

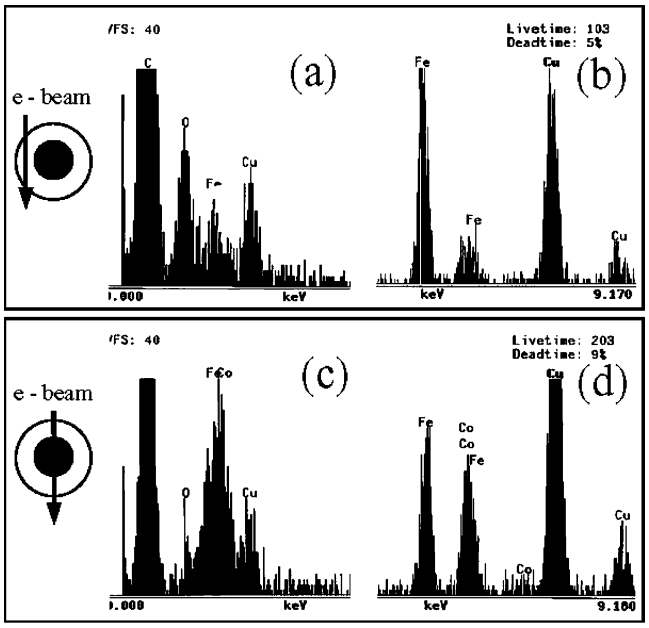

Figure 4. Comparison of the EDS spectra (displayed for different energy ranges) acquired from (a, b) the shell and (c, d) the core of a core−shell nanoparticle. The core is significantly rich in Co, but poor in oxygen.

positioning the electron probe through only the shell and through the core and shell, respectively. The spectra are displayed for different energy ranges. The copper and carbon signals came from the TEM grid. It is apparent that the shell is dominated by Fe, while the core is rich in Co, suggesting that the shell of the large-size nanoparticle is Fe_3O_4. It is, however, uncertain if the core is the $CoFe_2O_4$ phase, although the EDS data show both Co and Fe signals (see Figures 4c and d).

Electron diffraction and HRTEM have been applied in conjunction to determine if the core is $CoFe_2O_4$. HRTEM images can provide important real-space structural information, but only the particles oriented along specific directions and the lattice planes that are large enough to be resolved by TEM can give rise to lattice fringes in the image. Electron diffraction patterns recorded from a large number of particles have a unique

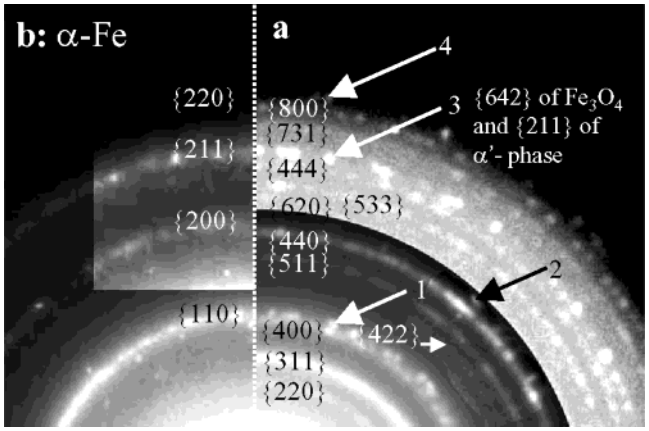

Figure 5. (a) Electron diffraction pattern recorded from core−shell nanoparticles for identifying the Spinel phase. (b) Electron diffraction pattern recorded from a standard sample of α-Fe nanocrystallites for identifying the four unknown diffraction rings, as labeled with arrowheads.

advantage, which is that all of the lattice planes are represented in the diffraction pattern. We can fit a wide range of diffraction peaks to uniquely determine the structure. Figure 5a shows an electron diffraction pattern recorded from an array of over 200 core−shell structured nanoparticles. Using the standard crystallographic data for Fe_3O_4, a set of diffraction rings (with the indexes) has been identified. However, there are three additional diffraction rings that remain to be identified. They are weak and noncontinuous and are labeled with arrowheads 1, 2, and 4. If the core is $CoFe_2O_4$ and the shell is Fe_3O_4, no additional diffraction would be observed in the diffraction pattern because both $CoFe_2O_4$ and Fe_3O_4 have an almost identical crystal structure and lattice parameters. The presence of additional peaks may suggest that the core could have a structure different from Spinel. The question now is what phase is this?

From the EDS data shown in Figure 4d, the core should contain both Co and Fe. From the binary Co−Fe phase diagram,[11] we found that, in a composition range (At%) of 29−75% of Fe, there exists a CoFe (α′) phase with an ordered CsCl structure (body centered cubic, *bcc*), with space group $Pm\bar{3}m$ (221) and lattice parameter $a = 2.857$ Å. The CoFe structure is almost identical to the *bcc*-structured α-Fe ($a = 2.86$ Å). Therefore, we may use the diffraction data recorded from α-Fe available to us to identify the unknown phase. A careful comparison of the electron diffraction pattern from the core−shell sample (Figure 5a) with the diffraction pattern recorded from α-Fe nanocrystals (Figure 5b) under identical experimental conditions shows that the additional three diffraction rings from the sample match the {110}, {200}, and {220} rings of the α-Fe phase, although the {220} ring of α-Fe is weak. It is also noted that the {211} rings of the α-Fe phase matches the {642} ring of the Fe_3O_4 phase. For the Fe_3O_4 phase, the *d* space of the {642} is 1.1214 Å, which is very close to the {211} *d*-space of the α-Fe phase ($d_{\{211\}} = 1.1676$ Å). Therefore, it is reasonable to believe that the diffraction ring corresponding to {642} of Fe_3O_4 overlaps with the {211} of α-Fe. Finally, the {110}, {200}, {211}, and {220} diffractions of the α-Fe match well to the unidentified diffraction rings that are labeled 1−4 in Figure 5a, respectively. As we discussed above, because the lattice parameters of the α-Fe phase and the CoFe (α′) phase are almost identical, it is suggested that the nanoparticles contain the CoFe (α′) phase. Due to a very low volume fraction of the core, the {100} and {111} diffraction rings from the CoFe (α′) are too weak to be observed. Table 1 lists the result of phase determination from electron diffraction data. The interplanar

TABLE 1: Phase Identification by Electron Diffraction Data

	d, measured ±0.05[a]	Miller indices		*d*, standard data[b]	
		Fe_3O_4	CoFe	Fe_3O_4	CoFe
1	2.93	{220}		2.966	
2	2.51	{311}		2.53	
3	2.08	{400}		2.096	
4	2.01*		{110}		2.0202
5	1.70	{422}		1.712	
6	1.61	{511}		1.614	
7	1.47	{440}		1.483	
8	1.43*		{200}		1.4285
9	1.33	{620}		1.327	
10	1.28	{533}		1.279	
11	1.21	{444}		1.2112	
12	1.16*	{642}	{211}	1.1214	1.1664
13	1.09	{731}		1.0922	
14	1.05	{800}		1.0489	
15	1.02*		{220}		1.0101

[a,b] Lengths of *d* are in Å. * Additional diffractions corresponding to the α′-CoFe phase.

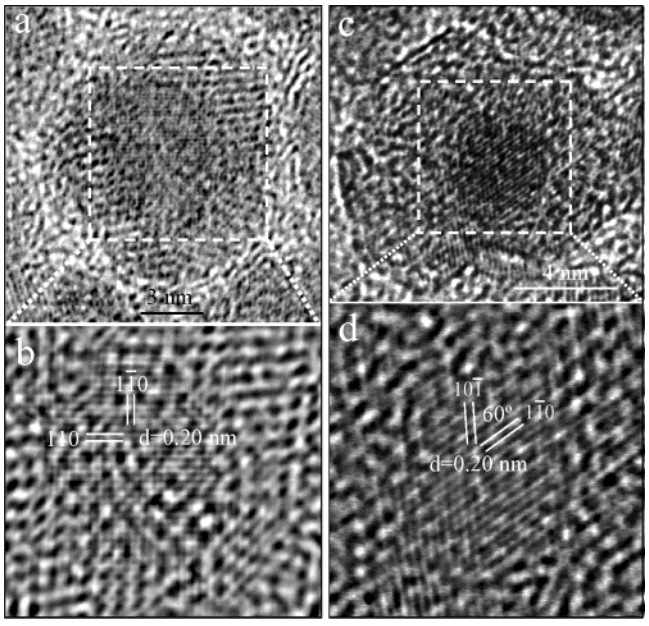

Figure 6. HRTEM images and the Fourier filtered images recorded from the cores of a core−shell nanoparticle that is oriented along (a, b) [001] and (c, d) [111]; the structure is identified to be CoFe (α′).

distances measured from the electron diffraction pattern and the standard data are compared in Table 1. The data confirmed that the CoFe (α′) phase exists in the nanoparticles, but its real space location has to be identified by imaging.

HRTEM helps to identify if the core is CoFe. As mentioned above, it is difficult to get an HRTEM image of the core with high quality because the cores are embedded in the polycrystalline shells of the nanoparticles with a thickness of ∼3 nm. In many cases, the cores show lattice fringes with a *d*-space of 2.02 Å, which corresponds to the {110} planes of CoFe (α′). Figure 6 shows HRTEM images recorded from the cores. Fourier filtering was used to extract the lattice fringe information by suppressing noise. HRTEM images with an incident beam along [001] (Figure 6a, Figure 6b) and [111] of the core are shown (Figure 6c, Figure 6d). The corresponding lattice planes are indexed to be the {110} type and their interplanar spacing matches well to that of CoFe. Therefore, the core has the α′-CoFe structure. On the other hand, because CoFe has a significantly higher volume density than Fe_3O_4 does, the core generates more scattering than the shell, resulting in darker contrast as observed in Figure 2.

In summary, this paper shows a conjunction application of high-resolution TEM, EDS microanalysis, and electron diffraction for determining the structure of core−shell nanoparticles. A detailed and systematic analysis found that the as-synthesized nanoparticles are the CoFe−Fe_3O_4 core−shell. This work shows the importance of quantitative structure analysis for the composite nanoparticles. The procedures and methodology presented here can be extended to the analysis of general nanoparticles that have a complex phase structure.

Acknowledgment. This work has been supported by U.S. DoD/DARPA through ARO under grant DAAD-19-01-1-0546.

References and Notes

(1) Danek, M.; Jensen, K. F.; Murray, C. B.; Bawendi, M. G. *Chem. Mater*. **1996**, *8*, 173.

(2) Dabbousi, B. O.; Rodriguez-Viejo, J.; Mikulec, F. V.; Heine, J. R.; Mattoussi, H.; Ober, R.; Jensen, K. F.; Bawendi, M. G. *J. Phys. Chem. B* **1997**, *101*, 9463.

(3) Peng, X.; Schlamp, M. C.; Kadavanich, A. V.; Alivisatos, A. P. *J. Am. Chem. Soc*. **1997**, *119*, 7019.

(4) Malik, M. A.; O'Brien, P.; Revaprasadu, N. *Chem. Mater*. **2002**, *14*, 2004.

(5) Reiss, P.; Bleuse, J.; Pron, A. *Nano Lett.* **2002**, *2*, 781.

(6) Hines, M. A.; Guyot-Sionnest, P. *J. Phys. Chem*. **1996**, *100*, 468.

(7) Skumryev, V.; Stoyanov, S.; Zhang, Y.; Hadjipanayis, G.; Givord, D.; Nogues, J. *Nature* **2003**, *423*, 850.

(8) Zeng, H.; Li, J.; Wang, Z. L.; Liu, J. P.; Sun, S. H. *Nano Lett.* **2004**, *4*, 187.

(9) Zeng, H.; Sun, S. H.; Li, J.; Wang, Z. L.; Liu, J. P. Submitted to *Appl. Phys. Lett*. **2004**.

(10) Sun, S.; Zeng, H.; Robinson, D. B.; Raoux, S.; Rice, P. M.; Wang, S. X.; Li, G. *J. Am. Chem. Soc*. **2004**, *126*, 273.

(11) Massalski, T. B.; Murray, J. L.; Bennett, L. H.; Baker, H. *Binary Alloy Phase Diagrams*; American Society for Metals: Ohio, 1986.